International Journal of Computational Methods and Experimental Measurements
Vol. 12, No. 4, December, 2024, pp. 403-410
Journal homepage: http://iieta.org/journals/ijcmem

Investigating Thinning and Wrinkling in Deep Drawing Processes: A Comparative Analysis of Two Punch Designs on 2.5 mm Aluminum Sheets

Agus Dwi Anggono*, Masyrukan, Agus Hariyanto, Farid Royani, Farid Firmansyah, Ahmad Avivudin Crismansyah

Department of Mechanical Engineering, Universitas Muhammadiyah Surakarta, Sukoharjo 57162, Indonesia

Corresponding Author Email: ada126@ums.id

Copyright: ©2024 The authors. This article is published by IIETA and is licensed under the CC BY 4.0 license (http://creativecommons.org/licenses/by/4.0/).

https://doi.org/10.18280/ijcmem.120409

Received: 19 September 2024
Revised: 25 November 2024
Accepted: 7 December 2024
Available online: 27 December 2024

Keywords:
sheet metal forming, deep drawing, punch model, aluminum 1050, Forming Limit Diagram (FLD), thinning and wrinkling

ABSTRACT

In order to minimize trial-and-error costs and avoid any faults throughout the production process, sheet metal forming is commonly used in the automotive industry to fabricate body pieces. This study examines how several punch models affect thinning and wrinkling during the deep drawing of aluminum 1050, a 2.50 mm thick material, under 150 KN of pressure. The Forming Limit Diagram (FLD) was used in the simulations to study material deformation and determine safe and essential places on the blank. According to the findings, die pressure-induced material stretching caused the material to significantly rise in major-minor strain, major-minor stress, thinning, and wrinkling by the fifth step. Additionally, for punch 1 material, the safe area grew from 9.20% to 49.36%; punch 2 increased from 9.08% to 46.85%. The non-linear FLD graph analysis verified that both materials stayed in the safe zone the entire time. These results demonstrate how well deep drawing simulations work to improve punch design and aluminum component performance in the automobile industry.

1. INTRODUCTION

Deep drawing is a crucial metal-forming process in the automotive industry, enabling the fabrication of complex-shaped components from sheet metal [1]. The right tooling design prevents defects such as thinning, wrinkling and springback during deep drawing. However, the process is susceptible to defects such as thinning and wrinkling, which can compromise the final product's (springback compensation) structural integrity and aesthetic appeal [2].

Researchers investigated wrinkles on the sidewall during deep drawing of the cylindrical cup in AA5042 aluminum alloy using finite element simulation and experimental measurements. A numerical model with accurate plastic anisotropy captured the wrinkle shape and location well, in agreement with experiments [2, 3].

Another study examined the effects of die and punch geometry on the thinning and wrinkling behavior during deep drawing of 2.5mm thick DP800 steel sheets. It was found that the thinning and wrinkling were significantly influenced by the die and punch radii, with smaller radii leading to more severe thinning and wrinkling [4].

The anisotropic plastic material was modelled with a yield criterion beyond the isotropic material behavior (von Mises). Accurate modeling of the plastic anisotropy of the aluminum alloy produced numerical results that were in good agreement with the experiments, especially the shape and location of the wrinkles [5]. The results showed that the wrinkle shape predicted by the numerical model was strongly influenced by the finite elements used in blank discretization. Accurate modeling of the plastic anisotropy of aluminum alloy produced numerical results that were in good agreement with the experiments, especially the shape and location of the wrinkles [6].

The researchers studied the last blank holder gap that can be used to avoid wrinkles and crack faults in T4 Tinplate CA rectangular cups. The designed standard tool was the basis for determining the punch-die dominance [7]. Analytical, finite element (FE), and experimental methodologies were used as the research methods. Every technique used in this research has been contrasted with other techniques. The study recommends a minimum blank holder gap of 120% to 130% of the original material thickness (about 0.24 ÷ 0.26 mm). The gap value guarantees that the wrinkle height remains minimum and the pulling force is maintained below the crucial threshold. It can inhibit the formation of wrinkles and cracks in the product [8, 9].

This study aims to investigate the impact of two distinct punch designs on the occurrence of these defects during the deep drawing of 2.5 mm thick aluminum sheets. Both finite element simulation and experiments were conducted in this research. The numerical simulations were performed using the Autoform finite element software package, widely used in the metal forming industry for simulating complex sheet metal forming processes such as deep drawing.

The numerical simulations showed that the punch design with a smaller radius led to more pronounced localized thinning in the sidewall region of the drawn component,

suggesting that the choice of punch geometry can significantly impact the thickness distribution within the part [4]. On the other hand, the use of a more considerable radius punch resulted in a more uniform thickness profile, potentially mitigating the risk of premature failure during subsequent forming or in-service loading [10].

The investigation also revealed that the selection of punch design influenced the onset and severity of wrinkling in the drawn component. Panels drawn with the smaller radius punch exhibited a greater tendency for wrinkling, particularly in the flange region. As the more abrupt deformation was imposed, the sharper tool geometry introduced increased compressive stresses in the material. Conversely, the more significant radius punch facilitated a more gradual deformation, reducing wrinkling propensity [11].

2. RESEARCH METHODOLOGY

The CAD-generated files were imported into forming simulation software for numerical analysis, as shown in Figure 1. Two punch models were proposed and investigated to examine their effects on thinning and wrinkling. In contrast, the original punch design featured a flat bottom zone in the centre. The simulations evaluated the performance and interactions of the components during deep drawing, offering insights into material behavior and optimizing punch and die design. The parameters used in the simulation are described in Table 1.

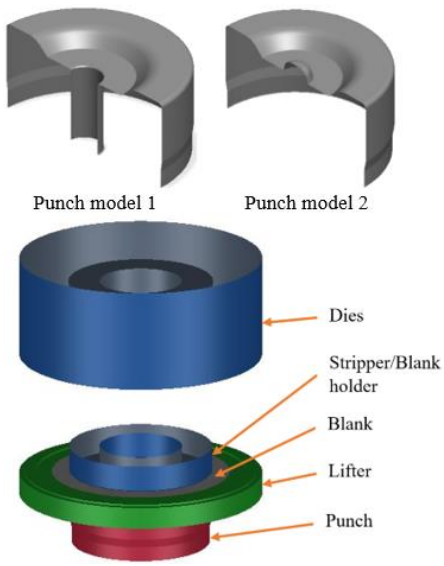

Figure 1. Punch model design and die set for simulation

The material used in this study is a pure aluminum plate with an aluminum composition of 99.50%, commonly called Alloy 1050. The properties of 1050 aluminum include a Young's Modulus of 71 GPa, yield stress of 110 MPa, tensile strength of 139.4 MPa, and a Poisson's ratio of 0.3. The thickness is 2.5 mm with a diameter of 246 mm and a force on the dies of 150 kN.

Aluminum sheets with a thickness of 2.5 mm are widely used in industries such as automotive, aerospace, and consumer goods due to their balance of structural integrity and lightweight properties, making them a practical choice for testing [12]. This thickness allows the evaluation of wrinkling behaviour during deep drawing under realistic conditions, avoiding extreme effects seen with thinner or thicker sheets. Applying a 150 kN force ensures effective deep drawing by balancing sufficient deformation, wrinkle suppression, and minimal thinning, reflecting both experimental constraints and industrial relevance, thereby producing robust and practically significant results [13].

The Forming Limit Diagram (FLD) analysis was conducted in five steps, each based on the distance between the dies and the punch. In step 1, the distance to the bottom was -40 mm, followed by -30 mm in step 2, -20 mm in step 3, and -10 mm in step 4. Finally, in step 5, the distance to the bottom reached 0.00 mm, marking the completion of the drawing process.

Table 1. Parameters in the forming simulation

Parameters	Value / Description
Dies	
Support Type	Force Controlled
Displacing Tool	Binder
Cushion Stroke	0.00 mm
Tool Stiffness	50 MPa/mm
Force/Pressure Constant Force	150 kN
Stripper	
Support Type	Spring Controlled
Displacing Tool	Punch
Cushion Stroke	650 mm
Tool Stiffness	50 MPa/mm
Force/Pressure Spring Stiffness	50 kN
Lifter	
Support Type	Force Controlled
Displacing Tool	Die
Cushion Stroke	50 mm
Tool Stiffness	50 MPa/mm
Force/Pressure Constant Force	75 kN
Punch	
Support Type	Rigid

3. RESULTS AND DISCUSSIONS

3.1 Forming limit diagram analysis on punch model 1

This study analysed the material behavior during the deep drawing process using punch model 1 through the Forming Limit Diagram (FLD) at various stages. The FLD was constructed based on experimental data obtained through Nakajima mechanical tests, which are widely used to determine the forming limits of sheet metal [14]. The FLD highly depends on material-specific properties, including thickness, anisotropy, and strain-hardening behaviour, ensuring its relevance to practical applications [15].

The Nakajima test involves deforming sheet metal specimens of varying widths using a hemispherical punch while recording strain distributions until failure occurs [16]. Different strain paths ranging from uniaxial tension to biaxial stretching are achieved by varying the specimen widths, providing comprehensive data on material behaviour under diverse loading conditions.

The construction of the FLD begins with data compilation, where strain data from each specimen are plotted on a graph with the major strain (ε_1) on the *y-axis* and the minor strain (ε_2) on the *x-axis* [17]. The failure points, corresponding to the onset of localized necking or tearing, are then connected to form the forming limit curve (FLC). This curve delineates safe strain combinations below the FLC from failure zones situated above the curve. The resulting FLD is a critical tool for

evaluating and optimizing forming processes [18].

The FLD curve in the first step of the process has a distance of -40 mm from the final drawing position. The thickening area showed a notable increase of 14.80%, indicating material accumulation due to compression, while the compression area reached 18.39%, reflecting localized stress concentrations. In contrast, the insufficiency in stretching, where the material does not extend adequately, was recorded at 57.61%. The stretching represents a considerable portion of the material undergoing insufficient stretching, which could lead to potential issues in uniformity and formability in the later stages of the process. The safe area, which represents the regions free from defects and within acceptable deformation limits, accounted for only 9.20%. This relatively small safe zone highlights the importance of precise process control to prevent defects [19]. These findings emphasize the importance of closely monitoring the process to mitigate potential defects as the forming operation progresses.

The second step of the process is positioned at -30 mm from the final drawing position. The thickening area increased to 17.30%, reflecting additional material buildup, while the compression area slightly decreased to 14.42%, potentially due to a redistribution of stresses. The insufficient stretch area dropped to 53.89%, indicating improved material elongation. The safe area grew to 14.39%, a positive development, although it still represented a relatively small portion of the material. As in the previous step, no changes were noted in the risk areas for splitting or thinning. The findings in this step suggest a progressive improvement in material formability, although continued attention to thickening and compression is necessary to ensure material integrity [20].

The third step is at a distance of -20 mm from the final drawing position. The thickening area was slightly reduced to 17.08%, indicating a stabilization in material buildup, while the compression area decreased to 13.00%, suggesting a more uniform distribution of stresses. The insufficient stretch area remained virtually unchanged at 53.90%, highlighting the need for continued process control to address formability challenges. The safe area increased to 16.03%, showing a gradual improvement in material behavior. Consistent with earlier steps, no risk areas for splitting or thinning were observed, indicating that the material remained within acceptable limits [21].

In the fourth step, the material showed further improvements at a distance of -10 mm from the final drawing position. The thickening area decreased to 17.02%, and the compression area reduced to 12.80%, reflecting a more balanced distribution of forces. The insufficient stretching area also saw a notable reduction to 46.74%, indicating better material adaptation to the drawing forces. The safe area increased significantly to 23.44%, representing a substantial portion of the material within safe deformation limits. No changes were observed in the risk areas for splitting or thinning, suggesting that the material remained stable under the applied forces. The data indicate a continued improvement in material behavior as the process neared its final stages [22].

Figure 2 illustrates the FLD curve for the fifth and final step of the deep drawing process, positioned at 0.00 mm from the base of the die. At this stage, the thickening area decreased slightly to 16.97%, indicating a stabilization of material buildup. The compression area reduced to 12.06%, continuing the more uniform force distribution trend. The insufficient stretching area decreased significantly to 21.61%, indicating that the material had effectively adapted to the drawing forces. The safe area expanded considerably to 49.36%, nearly half of the total material, highlighting the process's success in maintaining material integrity and minimizing defects. Importantly, no changes were observed in the risk areas for splitting, thinning, or other critical failures, indicating that the material did not reach essential thresholds for failure.

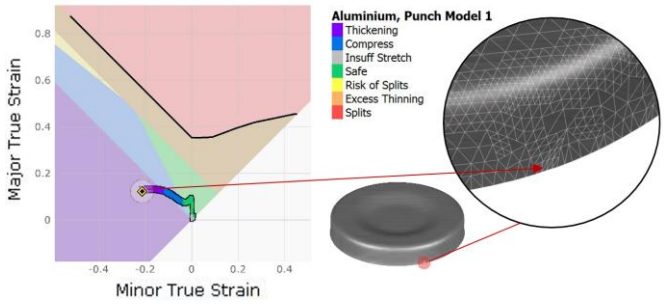

Figure 2. FLD in the final step

The deep drawing process demonstrated a progressive improvement in material behavior, with reductions in thickening, compression, and insufficient stretching, and a significant expansion in the safe area as the process progressed from step 1 to step 5. The absence of splitting or excessive thinning throughout the process underscores the success of the forming operation in maintaining material integrity and preventing defects. These findings highlight the importance of balancing forces and controlling deformation throughout the deep drawing process to ensure high-quality outcomes [23].

3.2 Forming limit diagram analysis on punch model 2

The analysis of material deformation using punch model 2 during the deep drawing process is detailed in Figure 3, showing changes in thickening, compression, stretching, and risk areas for splitting and thinning across different stages. In the initial stage, at a distance of -40 mm, the thickening area was 14.82%, and compression was 18.38%, with 57.72% of the material under-stretched. The safe area remained small at 9.08%, indicating potential risks if adjustments were not made. By the second stage of -30 mm, thickening increased to 17.30%, while compression slightly decreased to 14.46%. The insufficiency stretch stayed high at 53.90%, though the safe area improved to 14.33%, yet risks from compression and under-stretching remained.

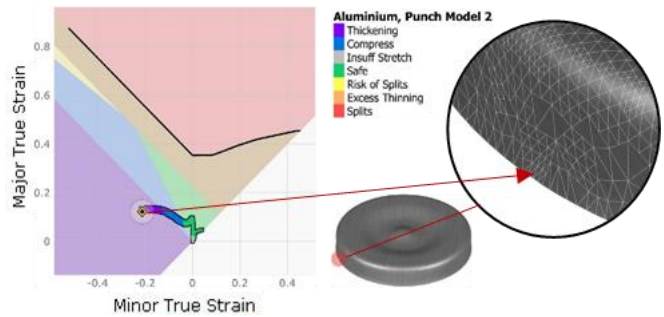

Figure 3. FLD in the final step for punch model 2

In the distance of -20 mm (third stage), thickening reduced slightly to 17.08%, and compression decreased further to 13.07%, with the safe area expanding to 15.95%. However, under-stretching remained significant at 53.91%. By the fourth

stage, thickening dropped to 16.97%, and compression reduced to 12.84%, while the safe area increased significantly to 28.67%, and the insufficient stretching area decreased to 41.52%. Despite these improvements, risks of thinning persisted. In the final stage (Figure 3), the thickening area was further reduced to 16.79%, and compression dropped to 11.95%. Insufficient stretch was decreased to 21.09%, and the safe area expanded dramatically to 46.85%. However, excess thinning increased by 3.32%, requiring close monitoring to maintain structural integrity.

The deep drawing process using punch model 2 demonstrated a clear progression in material behavior, with reductions in thickening, compression, and under-stretching as the process advanced. However, thinning and splitting risks persisted, highlighting the need for optimization in punch velocity, lubrication, and die clearance to ensure a defect-free final product.

Table 2 shows that there is no significant difference in the thickening and compression areas from Step 1 to Step 5 because both punch models share similar characteristics in the outer radius area. The highest thickening area was observed in step 2 for both punch models, measuring 17.30%, followed by a gradual decrease to 16.97% for punch model 1 and 16.79% for punch model 2 by step 5, contributing to the material's thinning.

The compression area consistently decreased from step 1 to step 5, reducing from 18.39% to 12.06% for punch model 1 and 18.38% to 11.95% for punch model 2. This reduction in the compression zone can lead to wrinkling in the aluminum material, particularly as the compressive forces diminish throughout the process.

As the forming process progressed, the insufficiency stress area also decreased, but a notable difference emerged in step 5, with punch model 1 showing 21.61% and punch model 2 exhibiting 21.09%. This slight variation in insufficient stretching indicates differences in how the material adapts to the punch force in the final stages.

Table 2. Material behavior during the forming process

Parameters	Step 1		Step 2		Step 3		Step 4		Step 5	
	1	2	1	2	1	2	1	2	1	2
Thickening (%)	14.8	14.82	17.3	17.3	17.08	17.08	17.02	16.97	16.97	16.79
Compress (%)	18.39	18.38	14.42	14.46	13	13.07	12.8	12.84	12.06	11.95
Insuff Stress (%)	57.61	57.72	53.89	53.90	53.90	53.91	46.74	41.52	21.61	21.09
Safe (%)	9.2	9.08	14.39	14.33	16.03	15.95	23.44	28.67	49.36	46.85
Risk of Split (%)	0	0	0	0	0	0	0	0	0	3.32

The safe material area expanded significantly from step 1 to step 5. For punch model 1, it increased from 9.20% to 49.36%, while for punch model 2, it rose from 9.08% to 46.58%. This substantial improvement in the safe area demonstrates that the material could increasingly deform within acceptable limits, reducing the risk of defects as the process advanced.

However, the risk of split area at step 5 for punch model 2 increased significantly to 3.32%. If not properly controlled, this elevated risk could result in material cracking (tearing), particularly in areas experiencing excessive thinning.

These observations highlight the importance of monitoring material behavior, especially in terms of thickening, compression, and the risk of splitting, to optimize the forming process and prevent defects in the final product.

3.3 Minor and major strain analysis

Figure 4 shows the evolution of minor strain during the deep drawing process from step 1 to step 5. The highest strain values occur at step 5, with punch model 1 reaching 0.059 and punch model 2 significantly higher at 0.179. This increase from step 4 to step 5 indicates growing deformation, with elevated strain areas posing a risk of cracking, particularly in punch model 2, where strain-induced failure is more likely. The difference between the two models highlights the importance of punch design in controlling strain distribution and stability, especially in the final stages of forming [24].

Figure 5 illustrates major strain behavior, showing no significant change for punch model 1 between steps 4 and 5, maintaining 0.139, while punch model 2 saw a sharp rise from 0.140 to 0.314. This increased strain in punch model 2 suggests intense deformation, with a higher risk of wrinkling due to uneven stress distribution. Wrinkling typically occurs in areas with excessive compressive forces, potentially compromising part quality. The contrast in strain behavior between the models emphasizes the role of punch geometry in influencing deformation and the need for careful punch design to minimize defects like wrinkling [25].

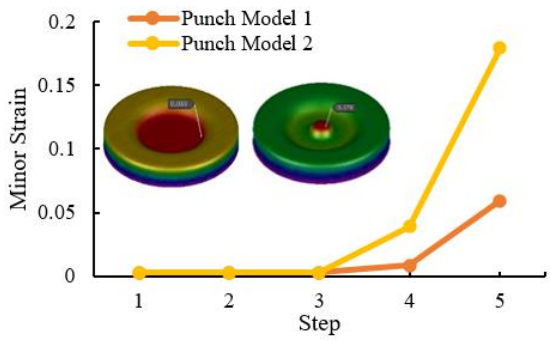

Figure 4. Minor strain in every step

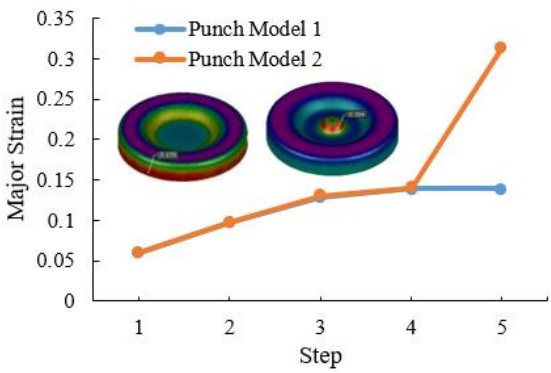

Figure 5. Major strain in every step

The higher risk of thinning and splitting observed in punch model 2 compared to punch model 1 was attributed to several

factors: punch model 2 has a smaller radius, leading to more pronounced localized thinning in the sidewall region of the drawn component, introducing higher localized stresses during the drawing process and resulting in more significant material deformation and thinning. The sharper geometry of punch model 2 imposes more abrupt deformation, introducing increased compressive stresses in the material, leading to a higher tendency for splitting, especially in areas experiencing excessive thinning. Punch model 2's design affects the material flow during the deep drawing process, causing uneven stress distribution and higher localized thinning, increasing the risk of splitting. The FLD analysis showed that punch model 2 exhibited higher minor and major strain values than punch model 1, indicating more significant deformation and a higher risk of cracking.

3.4 Minor and major stress analysis

As shown in Figure 6(a), minor stress analysis across five stages of the deep drawing process revealed a decrease in stress at step 3, with values of 34.37 MPa for punch model 1 and 35.31 MPa for punch model 2. However, a significant increase was observed from steps 4 to 5, peaking at 93.42 MPa (punch model 1) and 123.3 MPa (punch model 2). This increase suggests heightened internal forces due to increased contact pressure and deformation. The higher stress in punch model 2 indicates more significant deformation and a higher risk of defects, highlighting the role of punch design in managing stress distribution and minimizing material failure risks. Monitoring minor stress, especially in later stages, is crucial to maintaining material integrity [26].

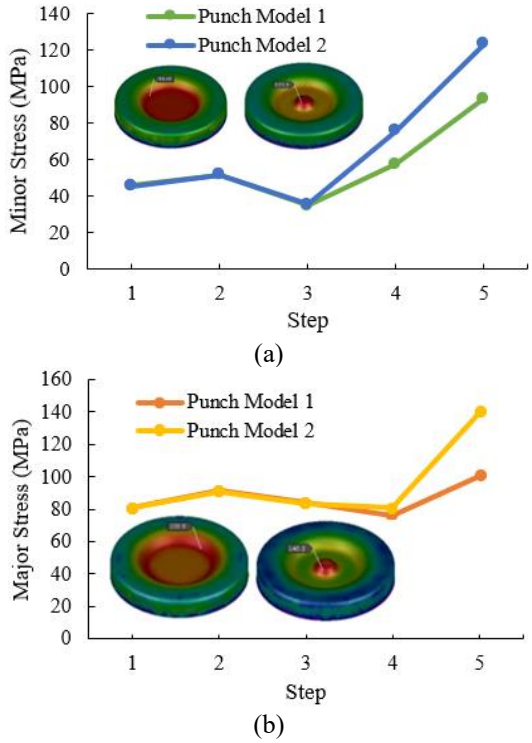

Figure 6. (a) Minor stress in every step, and (b) major stress in every step

Similarly, as shown in Figure 6(b), major stress analysis reduced from 91.62 MPa to 76.31 MPa (punch model 1) and from 91.08 MPa to 80.96 MPa (punch model 2) between steps 3 and 4. In step 5, major stress increased significantly to 100.9 MPa for punch model 1 and 140.2 MPa for punch model 2. The more considerable rise in model 2 indicates more concentrated forces, increasing the risk of wrinkling or tearing. The force underscores the importance of managing stress levels, particularly in the final stages, to avoid overstressing the material and compromising product quality.

The significant increase in minor and major stresses during the final stage of the deep drawing process for punch model 2 is primarily due to its smaller radius. This geometry results in localized deformation, higher stress concentrations, and greater resistance as the material is drawn into the die. Additionally, the smaller radius disrupts material flow, leading to uneven stress distribution. Increased friction at the punch-material interface, potentially exacerbated by the smaller radius, further amplifies stress levels. Factors like higher drawing speeds and reduced die clearance associated with punch model 2 also contribute to the observed stress escalation.

3.5 Thinning and wrinkling analysis

Figure 7 presents the thinning analysis of 2.5 mm thick aluminum material using two punch models, showing progressive thinning as the deep drawing process advanced from step 1 to step 5. In punch model 1, thinning was measured at 0.156 mm, whereas punch model 2 exhibited significantly greater thinning, reaching 0.353 mm. The more pronounced thinning in punch model 2 indicates that it induces higher localized stresses during the drawing process, resulting in more significant material deformation.

The excessive thinning observed in punch model 2 raises concerns about the potential reduction in structural integrity, as thinner sections of the material become more vulnerable to failure under mechanical load or stress. This finding underscores the importance of selecting the appropriate punch geometries and optimizing process parameters—such as punch force, drawing speed, and lubrication conditions—to minimize localized stresses and ensure the material maintains its durability and strength throughout the forming process.

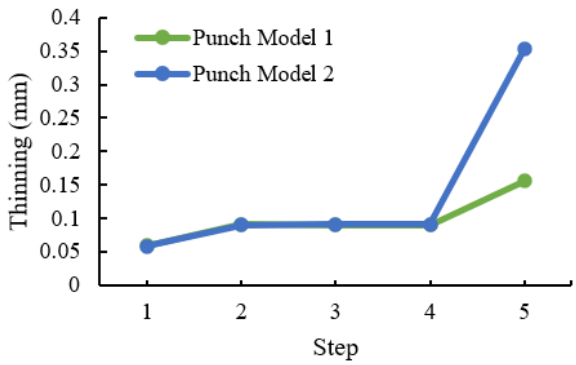

Figure 7. Result of thinning in every steps

Thinning beyond acceptable limits could compromise the performance of the aluminum component in practical applications, making it crucial to implement careful control measures in the deep drawing process. Adjustments in punch design, die clearance, and material flow management are critical to preventing excessive thinning and ensuring a consistent final product with sufficient thickness and strength for long-term reliability [27].

Figure 8 illustrates the wrinkling observed during the deep drawing process, with wrinkled areas highlighted in red. Both

punch models exhibited similar wrinkling behavior, with a final wrinkling value of 0.041 mm and a peak wrinkling of 0.055 mm at step 4. This consistency in wrinkling suggests that the geometry of the outer diameter of the punches plays a significant role in the formation of wrinkles during the drawing process. The influence of the punch geometry on material flow and the distribution of compressive forces is critical in determining the extent of wrinkling.

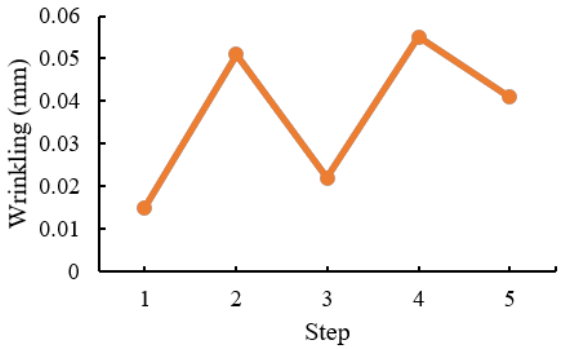

Figure 8. Result of wrinkling in every steps

Although the wrinkling values are relatively low, controlling this defect is essential for ensuring the final product's surface finish and dimensional accuracy. Wrinkling can negatively affect the aesthetic and structural qualities of the formed aluminum parts, potentially leading to surface imperfections and geometric deviations that may impact the part's performance in practical applications. To minimize wrinkling, optimising several factors, including punch design carefully, die clearance, and overall process parameters such as drawing speed, lubrication, and material handling is essential.

The simulation considered two lubrication conditions: lubricated and unlubricated, with coefficients of friction (CoF) set at 0.05 and 0.15, respectively. Conversely, in the experimental setup, the CoF for the aluminum-steel interface ranged between 0.3 and 0.5. A higher CoF significantly increases frictional resistance, restricts material flow, and leads to localized thinning and a greater susceptibility to failure through tearing. Moreover, in the context of wrinkling, elevated CoF values promote material accumulation in the flange region, inducing compressive stresses that form wrinkles [28].

By fine-tuning these variables, the risk of wrinkling can be significantly reduced, resulting in improved material flow and a smoother surface finish. In doing so, manufacturers can enhance the quality and precision of the formed aluminum components, ensuring that they meet the required industrial-use specifications. Moreover, reducing wrinkling improves dimensional accuracy and contributes to process efficiency, minimizing material waste and the need for post-processing corrections [29].

The structural integrity and practical performance of aluminum components were seriously compromised by excessive thinning. Overly thin portions were more prone to failure mechanisms including cracking, tearing, or, in extreme situations, total structural collapse under operating conditions because they were less able to bear mechanical loads and stresses. Additionally, thinner areas were more susceptible to fatigue, which shortened their lifespan and compromised their dependability. Excessive thinning has led to catastrophic failures in dynamic load applications, especially in the automotive and aerospace industries, posing significant safety issues. In order to guarantee the longevity, mechanical strength, and general dependability of aluminum components in harsh operating situations, it was crucial to maintain an ideal material thickness.

4. CONCLUSIONS

This study simulated the deep drawing of aluminum 1050 using two different punch models, revealing several key findings. For punch model 1, the safe area increased progressively from 9.20% in step 1 to 49.36% in step 5. Minor-major strain rose steadily, while major strain stabilized at 0.139 by step 5. Minor stress decreased to 34.73 MPa in step 3 before rising to 93.42 MPa in step 5. Major stress followed a similar trend, decreasing from 91.65 MPa to 76.31 MPa between steps 3 and 4, then rising to 100.9 MPa in step 5, posing a risk of cracking in the aluminum material. In punch model 2, the safe area expanded from 9.08% to 46.85%. Minor-major strain increased significantly as the process progressed, with minor stress dropping to 35.31 MPa in step 3, then rising to 123.3 MPa by step 5. Major stress decreased from 91.08 MPa to 80.96 MPa before increasing sharply to 140.2 MPa in step 5, indicating a higher potential for cracking in risk areas. Additionally, thinning increased from 0.059 mm to 0.156 mm for punch model 1 and from 0.058 mm to 0.353 mm for punch model 2, while both models showed wrinkling of 0.041 mm at the outer diameter by the end of the process.

The results demonstrate significant strain, stress, thinning, and wrinkling differences between the punch models. These findings emphasize the importance of optimizing punch design and process parameters to minimize defects such as thinning, wrinkling, and cracking, thereby improving the quality and performance of aluminum components in industrial applications.

ACKNOWLEDGMENT

The authors express their gratitude to Universitas Muhammadiyah Surakarta through the Innovation and Research Office for their substantial financial assistance in the study project under the Doctoral Competency Scheme, contract number. 125.37/A.3-III/LRI/IV/2024. They would like to thank the Mechanical Engineering Department and Material Laboratory of Universitas Muhammadiyah Surakarta for their significant contributions to the project.

REFERENCES

[1] Do, T.T., Minh, P.S., Le, N. (2021). Effect of tool geometry parameters on the formability of a camera cover in the deep drawing process. Materials, 14(14): 3993. https://doi.org/10.3390/ma14143993

[2] Mastrone, M.N., Concli, F. (2023). Implementation of a numerical model for the prediction of aeration in mechanical systems. International Journal of Computational Methods and Experimental Measurements, 11(2): 65-71. https://doi.org/10.18280/ijcmem.110201

[3] Yahya, I.Z.A., Kaedhi, H.M., Karash, E.T., Najm, W.M. (2024). Finite element analysis of the effect of carbon

nanotube content on the compressive properties of zirconia nanocomposites. International Journal of Computational Methods and Experimental Measurements, 12(3): 227-235. https://doi.org/10.18280/ijcmem.120304

[4] Anggono, A.D., Siswanto, W.A., Omar, B., Yulianto, A. (2024). Advancing die design and optimization through the combination approach: A focus on spring-back compensation. International Journal of Mathematical, Engineering & Management Sciences, 9(2): 205-223. https://doi.org/10.33889/IJMEMS.2024.9.2.011

[5] Jung, D.K., Ha, S.H., Kim, H.K., Shin, Y.C. (2021). Determination of plastic anisotropy of extruded 7075 aluminum alloy thick plate for simulation of post-extrusion forming. Metals, 11(4): 641. https://doi.org/10.3390/met11040641

[6] Darmawan, A.S., Anggono, A.D., Hamid, A. (2018). Die design optimization on sheet metal forming with considering the phenomenon of springback to improve product quality. MATEC Web of Conferences, 154: 01105. https://doi.org/10.1051/matecconf/201815401105

[7] Li, J., Chen, X., Liu, X. (2021). Investigation of process parameters and plate local thickening on residual stresses in hot stamping process. Mechanics & Industry, 22: 18. https://doi.org/10.1051/meca/2021015

[8] Riyadi, T.W.B., Ahmad, F.H., Veza, I., Darmawan, A.S., Anggono, A.D., Purbolaksono, J. (2019). Study of the creep deformation of Sanicro 25 austenitic steel by computer simulations. Materials Science Forum, 96: 156-162. https://doi.org/10.4028/www.scientific.net/MSF.961.156

[9] Wang, Y., Lai, H., Cheng, Z., Zhang, H., Liu, Y., Jiang, L. (2019). Smart superhydrophobic shape memory adhesive surface toward selective capture/release of microdroplets. ACS Applied Materials & Interfaces, 11(11): 10988-10997. https://doi.org/10.1021/acsami.9b00278

[10] Vairavan, H., Abdullah, A.B. (2017). Die-punch alignment and its effect on the thinning pattern in the square-shaped deep drawing of aluminium alloy. International Journal of Materials and Product Technology, 54(1-3): 147-164. https://doi.org/10.1504/ijmpt.2017.080565

[11] Bergs, T., Nick, M., Feuerhack, A., Trauth, D., Klocke, F. (2018). Numerical-experimental investigation of load paths in DP800 dual phase steel during Nakajima test. AIP Conference Proceedings, 1960(1): 160021. https://doi.org/10.1063/1.5035047

[12] Ma, M.T., Zhang, J.P., Zhou, J., Lu, H.Z. (2018). Property requirements and research progress of aluminum alloy sheets for automotive closure. Materials Science Forum, 91: 18-29. https://doi.org/10.4028/www.scientific.net/msf.913.18

[13] Briesenick, D., Liewald, M. (2022). Multistage deep-drawing with alternating blank draw-in for Springback reduction in transfer and progressive dies. Key Engineering Materials, 926: 674-682. https://doi.org/10.4028/p-25ow1x

[14] Schwindt, C.D., Stout, M., Iurman, L., Signorelli, J.W. (2015). Forming limit curve determination of a DP-780 steel sheet. Procedia Materials Science, 8: 978-985. https://doi.org/10.1016/j.mspro.2015.04.159

[15] Rubešová, K., Rund, M., Rzepa, S., Jirková, H., et al. (2021). Determining forming limit diagrams using sub-sized specimen geometry and comparing FLD evaluation methods. Metals, 11(3): 484. https://doi.org/10.3390/met11030484

[16] Ayachi, N., Guermazi, N., Pham, C.H., Manach, P.Y. (2020). Development of a nakazima test suitable for determining the formability of ultra-thin copper sheets. Metals, 10(9): 1163. https://doi.org/10.3390/met10091163

[17] Singh, P.K., Sarkar, R.B., Raj, A., Verma, R.K. (2017). Forming limit diagram generation with reduced experiments and modelling for different grades of automotive sheet steel using CrachLab. The Journal of Strain Analysis for Engineering Design, 52(5): 298-309. https://doi.org/10.1177/0309324717714095

[18] Stoughton, T.B., Carsley, J.E., Min, J., Lin, J. (2016). Advances in characterization of sheet metal forming limits. Journal of Physics: Conference Series, 734(3): 032073. https://doi.org/10.1088/1742-6596/734/3/032073

[19] Zhang, J., Xu, Y., Hu, P., Zhao, K. (2015). Development and applications of forming-condition-based formability diagram for split concerns in stamping. Journal of Manufacturing Processes, 17: 151-161. https://doi.org/10.1016/j.jmapro.2014.09.001

[20] Fan, X., Sun, B., Qu, W., Chen, X., Wang, X. (2023). Wrinkling and strengthening behaviors in the two-layer-sheet hot-forming-quenching integrated process for an Al-Cu-Mg-Alloy thin-walled curved-surface shell. Materials, 16(13): 4766. https://doi.org/10.3390/ma16134766

[21] Mo, C., Xu, Y., Yuan, S. (2023). Research on hydroforming of 5A06 aluminum alloy semi-ellipsoid shell with differential thickness. The International Journal of Advanced Manufacturing Technology, 125(1): 603-612. https://doi.org/10.1007/s00170-022-10749-4

[22] Moser, N., Leem, D., Ehmann, K., Cao, J. (2021). A high-fidelity simulation of double-sided incremental forming: Improving the accuracy by incorporating the effects of machine compliance. Journal of Materials Processing Technology, 295: 117152. https://doi.org/10.1016/j.jmatprotec.2021.117152

[23] Nezamaev, A.V., Karzhavin, V.V. (2020). Deep drawing failure modes. IOP Conference Series: Materials Science and Engineering, 966(1): 012126. https://doi.org/10.1088/1757-899x/966/1/012126

[24] Wang, W., Li, M., Zhao, Y., Wei, X. (2014). Study on stretch bendability and shear fracture of 800 MPa dual phase steel sheet. Materials & Design, 56: 907-913. https://doi.org/10.1016/j.matdes.2013.12.004

[25] Dal, S.R., Darendeliler, H. (2022). Analysis of side-wall wrinkling in deep drawing processes. Key Engineering Materials, 926: 732-743. https://doi.org/10.4028/p-i5q886

[26] Yao, P.P., Wang, Q. (2017). Investigation on hole punching process with combined punch to improve surface quality during the materials forming process. Key Engineering Materials, 737: 77-82. https://doi.org/10.4028/www.scientific.net/kem.737.77

[27] Siswanto, W.A., Anggono, A.D., Omar, B., Jusoff, K. (2014). An alternate method to springback compensation for sheet metal forming. The Scientific World Journal,

2014(1): 301271. https://doi.org/10.1155/2014/301271
[28] Chen, K., Carter, A.J., Korkolis, Y.P. (2022). Flange wrinkling in deep-drawing: Experiments, simulations and a reduced-order model. Journal of Manufacturing and Materials Processing, 6(4): 76. https://doi.org/10.3390/jmmp6040076
[29] Loganathan, C., Narayanasamy, R. (2008). Wrinkling behaviour of different grades of annealed commercially pure aluminium sheets when drawing through a conical die. Materials & Design, 29(3): 662-700. https://doi.org/10.1016/j.matdes.2006.04.009